Two-Carbon-Elongated HIV-1 Protease Inhibitors with a Tertiary-Alcohol-Containing Transition-State Mimic[⊥]

Xiongyu Wu,[†] Per Öhrngren,[†] Jenny K. Ekegren,[†] Johan Unge,[‡] Torsten Unge,[‡] Hans Wallberg,[§] Bertil Samuelsson,[§] Anders Hallberg,[†] and Mats Larhed*[,†]

Department of Medicinal Chemistry, Organic Pharmaceutical Chemistry, BMC, Uppsala University, Box 574, SE-751 23 Uppsala, Sweden, Department of Cell and Molecular Biology, Structural Biology, BMC, Uppsala University, Box 596, SE-751 24 Uppsala, Sweden, and Medivir AB, Lunastigen 7, SE-141 44, Huddinge, Sweden

Received June 12, 2007

A new generation of HIV-1 protease inhibitors encompassing a tertiary-alcohol-based transition-state mimic has been developed. By elongation of the core structure of recently reported inhibitors with two carbon atoms and by varying the P1′ group of the compounds, efficient inhibitors were obtained with K_i down to 2.3 nM and EC_{50} down to 0.17 μM. Two inhibitor−enzyme X-ray structures are reported.

Introduction

The devastating effects of the HIV/AIDS pandemic on individuals and entire countries are well-known. Despite this, the disease continues to spread and millions of lives are claimed every year.[1] One of the most important contributions to the arsenal of HIV drugs, lowering the viral plasma loads although not curing the infection, are the HIV-1 protease inhibitors.[2–4] In combination with other HIV drugs, the protease inhibitors provide prolonged lifetime and better quality of life for the patients. There are, however, certain issues that need to be addressed to improve the clinical efficacy of this class of drugs. Most of the launched HIV-1 protease inhibitors (to date nine compounds) exhibit low aqueous solubility, poor membrane permeability, high protein binding, and insufficient metabolic stability resulting in poor pharmacokinetic properties. Thus, high doses of drugs are needed and poor patient compliance is commonly observed.[3,5] Further, fast viral replication and a high number of errors made during viral transcription of RNA to DNA create a large amount of mutated viral strains. Resistance toward the launched protease inhibitors is a serious threat to efficient HIV treatment,[6,7] and the need for new, unique structural entities is therefore highly desirable.

In our ongoing efforts on the identification of novel HIV protease inhibitors, we recently described a new class of compounds with a shielded tertiary alcohol in the transition-state mimicking scaffold, as exemplified by **A** and **B** in Figure 1.[8–10] Despite an unsymmetrical arrangement of the tertiary alcohol over the two catalytically active aspartic acid residues in the enzyme as deduced by X-ray crystallography,[8,9] high enzyme inhibition activities were obtained. In addition, excellent permeation through a Caco-2 cell membrane was recorded for several compounds in this series.[8,9] We decided to further elaborate the core structure of these inhibitors and to elongate the distance between the tertiary alcohol and the hydrazide part of the molecules. A straightforward synthetic procedure, yielding two-carbon-elongated analogues with different P1′ substituents,

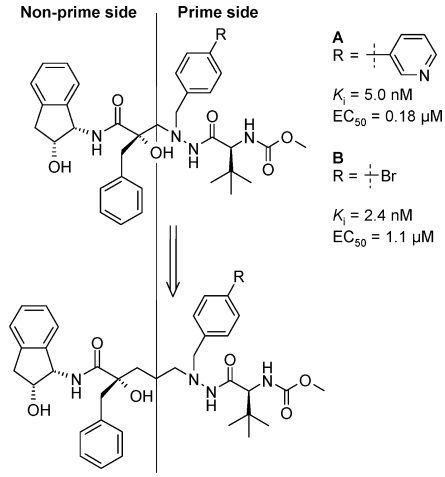

Figure 1. Structure and inhibition data for the best compound in the first generation of shielded inhibitors (**A**, top) with structure and inhibition data for the bromobenzene analoge (**B**, top). The bottom compound is the general structure of the new two-carbon-elongated scaffold.

was developed starting from commercially available 2-hydroxy-3-phenylpropionic acid. We herein present the new protocol, the biological evaluation, and X-ray data obtained from two compounds cocrystallized with the enzyme.

Results

Chemistry. A nonprime side building block, facilitating synthesis of the new two-carbon extended transition-state mimic, was prepared starting from the commercially available (*S*)-2-hydroxy-3-phenylpropionic acid (**1**) (Scheme 1). First, the alcohol and acid functionalities in **1** were protected using 2,2-dimethoxypropane as described in the literature,[11] followed by LDA[a] -mediated alkylation with methyl acrylate. Subsequent deprotection of the dioxolane in **3**, causing intramolecular lactone formation with the methyl ester, and peptide coupling

[⊥] PDB codes for structures **12d**, **15**, and **B** are 2uxz, 2uy0, and 2bqv, respectively.

* To whom correspondence should be addressed. Phone: +46-18-4714667. Fax: +46-18-4714474. E-mail: Mats.Larhed@orgfarm.uu.se.
[†] Department of Medicinal Chemistry, Uppsala University.
[‡] Department of Cell and Molecular Biology, Uppsala University.
[§] Medivir AB.

[a] Abbreviations: LDA, lithium diisopropylamide; EDC, 1-(3-dimethylamiopropyl-3-ethylcarbodiimide hydrochloride; HOBT, 1-hydroxybenzotriazole; TBSOTf, *tert*-butyldimethylsilyl trifluoromethanesulfonate; TBAF, tetrabutylammonium fluoride; TsOH, *p*-toluenesulfonic acid; XTT, a tetrazolium salt used in the colorimetric assay; RPMI, Roswell Park Memorial Institute (cell culture media).

10.1021/jm070680h CCC: $40.75
Published on Web 01/24/2008

Scheme 1. Synthesis of Nonprime Side Building Block (*R*)-**6**[a]

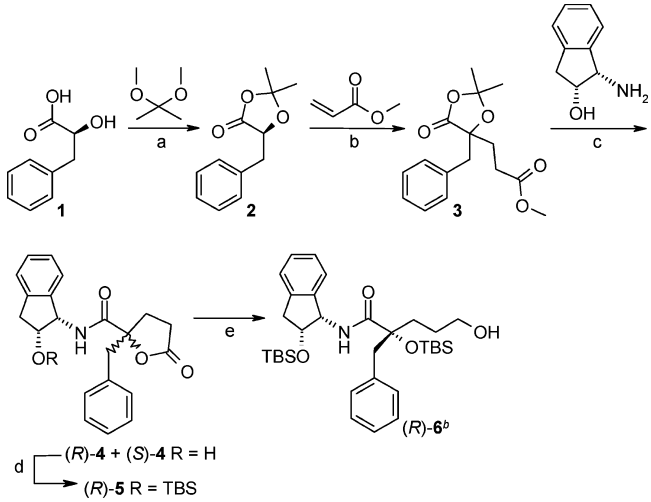

[a] Reagents and conditions: (a) pyridinium *p*-toluenesulfonate, $CHCl_3$, 70 °C, 97%; (b) LDA, −78 °C, THF, 54%; (c) (1) TFA, H_2O, 80 °C; (2) EDC, HOBT, CH_2Cl_2, room temp, 41% ((*R*)-**4**), 46% ((*S*)-**4**), separated by column chromatography; (d) TBSOTf, Et_3N, CH_2Cl_2, 0 °C to room temp, 92%; (e) (1) $LiBH_4$, Et_2O, 0 °C; (2) trimethylacetyl chloride, pyridine, room temp; (3) TBSOTf, Et_3N, CH_2Cl_2, 0 °C to room temp; (4) $LiBH_4$, Et_2O, room temp, 73%. [b] (*S*)-**6** was prepared from (*S*)-**4** according to a slightly modified procedure; see Supporting Information.

with (1*S*,2*R*)-1-amino-2-indanol gave cyclic **4** as a mixture of diastereomers (Scheme 1). Compounds (*R*)-**4** and (*S*)-**4** (*R* and *S* refer to the absolute configuration at the quaternary carbon and were determined by X-ray crystallography of (*S*)-**4**) were efficiently separated by column chromatography (see Supporting Information). Diastereomer (*R*)-**4**, exhibiting the preferred stereochemistry at the quaternary carbon as deduced from the previous series of inhibitors, was protected using TBSOTf. Finally, reduction of the lactone moiety, protection of the primary alcohol using trimethylacetyl chloride, protection of the tertiary alcohol with TBSOTf, and reduction of the trimethylacetyl ester with $LiBH_4$ gave alcohol (*R*)-**6** (Scheme 1).

On the prime side of the inhibitors, the L-*tert*-leucine P2′ group and P3′ methyl carbamate, known in related systems to yield inhibitors with good properties in cell-based assays, were chosen.[8,9,12] We were, however, interested to further explore the effects of different alkyl, aryl, and biaryl components in P1′, and a diverse set of hydrazides was synthesized (Scheme 2). Reductive amination of primary hydrazide **8**, prepared according to a literature procedure,[12] with various aldehydes resulted in β-nitrogen-alkylated **9a**–**r** encompassing small to large P1′ precursor groups with different polarity and hydrogen-bonding potential (Scheme 2). In the case of 4-iodobenzyl as the P1′ group, the reported methodologies starting from the corresponding 4-iodobenzyl bromide, hydrazine hydrate,[13] and free acid **11**[12] were used to afford hydrazide **9s** (Scheme 2).[8]

Inhibitors **12a**–**s** were obtained via oxidation of (*R*)-**6** using Dess−Martin periodinane and then reductive amination of the corresponding aldehyde with hydrazides **9a**−**s** (Scheme 3). The role of the free alcohols in inhibiting the HIV-1 protease was investigated by preparation of the TBS-protected compounds **13** and **14**, **13** with both the secondary and the tertiary alcohol protected and **14** with only the tertiary alcohol moiety protected (Scheme 3). In addition, derivative **13** was used in microwave-accelerated palladium-catalyzed Suzuki reactions, yielding P1′ biaryl-containing inhibitors **12t**–**w** (Scheme 3).[14–17] The corresponding acid of (*R*)-**6**, ((*R*)-**6**-acid) was synthesized by a two-step oxidation procedure and then coupled to hydrazide **9d** using

Scheme 2. Synthesis of Hydrazides **9a**–**s**[a]

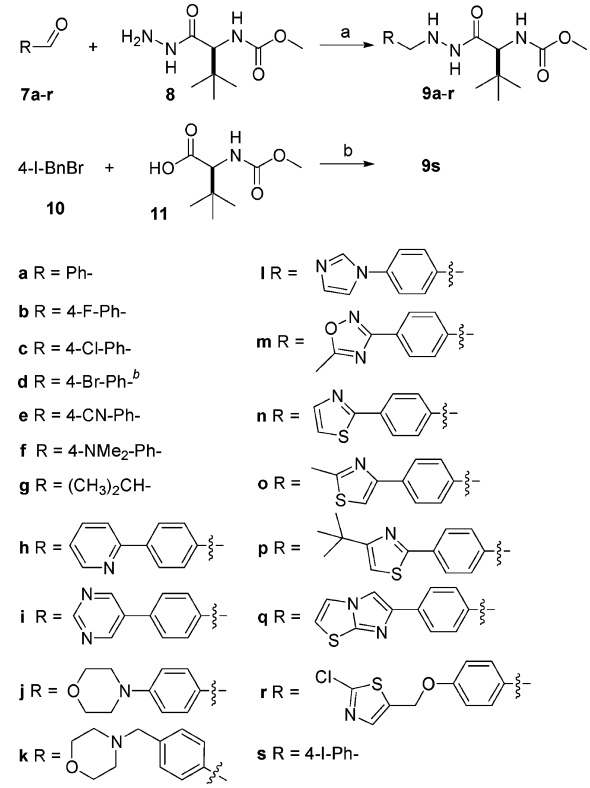

[a] Reagents and conditions: (a) (1) TsOH, $NaBH_3CN$, THF, room temp, 6–85%; (b) (1) hydrazine hydrate, EtOH, 0 °C to room temp; (2) **11**, EDC, HOBT, CH_2Cl_2, room temp, 15%. [b] **9d** was synthesized according to a published procedure.[8]

EDC and HOBT at room temperature, yielding diacylhydrazine derivative **15** (Scheme 3).

Biological Evaluations. The antiviral activities of **12a**–**w** and **13**−**15** are summarized as K_i and EC_{50} values in Table 1; previously published inhibitor **A** (Figure 1) is included as a reference compound.[9] All derivatives having the new prolonged transition-state mimic with *R*-configuration at the tertiary alcohol and free hydroxyl groups efficiently inhibited the HIV-1 protease (K_i = 2.4–11 nM, Table 1) except **12p** with a *tert*-butyl substituted thiazole group in P1′, which gave a higher K_i (24 nM, Table 1). The TBS-protected compounds **13** and **14**, as well as diacylhydrazine analogue **15**, were active in the enzyme assay but at high concentrations (980, 190, and 120 nM, Table 1). As expected from the previous class of HIV-1 protease inhibitors, (*S*)-**12d** was more than 100 times less active than the corresponding *R*-isomer.[8] A higher intercompound variability was recorded for the cellular (EC_{50}) anti-HIV activities. All inhibitors encompassing small P1′ groups, with –H, the halogens, –CN, and dimethylamine in the 4-position of the P1′ benzyl group (**12a**–**f**, Table 1) and the compounds on the other extreme, with large and/or very lipophilic P1′ groups, **12g**,**k**,**p**,**s**,**t**, gave poor inhibitory potencies with EC_{50} between 0.78 and 1.8 μM (Table 1). Compounds including the medium size 2-pyridyl, morpholine, methylthiazole, and thiophene 4-substituted inhibitors **12h**, **12j**, **12o**, and **12w**, as well as bicycle **12q**, were positioned at intermediate activities in the cell-based assay with EC_{50} between 0.47 and 0.56 μM (Table 1). Inspired by a published structure from GlaxoSmithKline,[19] the 2-chloro-5-methoxythiazole **12r** was made, but disappointingly no improvement in cell activity was observed for this inhibitor, which only showed intermediate potency, EC_{50} = 0.60 μM. The most potent compounds within this series, from 0.17

Scheme 3. Synthesis of Inhibitors **12a–w** and **13−15**[a]

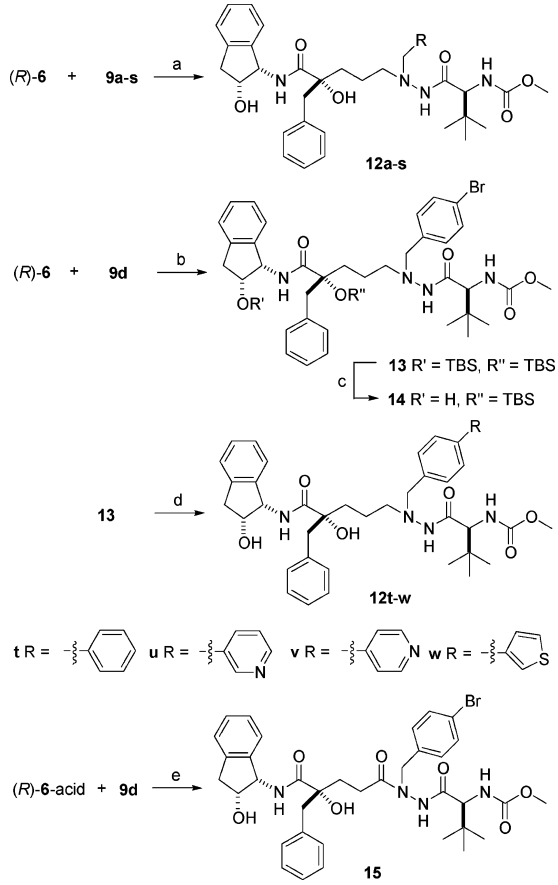

[a] Reagents and conditions: (a) (1) Dess−Martin periodinane, CH_2Cl_2, room temp; (2) **9a–s**, $Na(OAc)_3BH$, AcOH, THF, room temp; (3) TBAF (10 equiv), THF, room temp, 19–91%; (b) Dess−Martin periodinane, CH_2Cl_2, room temp; (2) **9d**, $Na(OAc)_3BH$, AcOH, THF, room temp, 48%; (c) TBAF (1 equiv), THF, room temp, 75%; (d) (1) boronic acid reactant, K_2CO_3, Herrmann's palladacycle,[18] $[(t\text{-}Bu)_3PH]BF_4$, DME/H_2O, irradiation in the microwave cavity for 20 min at 120 or 130 °C; (2) TBAF (10 equiv), THF, room temp, 61–80%; (e) EDC, HOBT, CH_2Cl_2, room temp, 39%.

to 0.22 μM in EC_{50}, were equipped with relatively hydrophilic aromatic groups containing two or three heteroatoms in the second P1′ aryl group or were pyridine analogues (**12i**,**l**−**n**,**u**,**v**, Table 1). Interestingly, the two inhibitors with 3-pyridyl (**12u**) and 4-pyridyl (**12v**) showed a 2.5-fold higher anti-HIV activity compared to the inhibitor with the 2-pyridyl (**12h**) which is the pyridyl used in atazanavir.[12] The CC_{50}, indicative of the inhibitor cytotoxicity, revealed that only two of the evaluated compounds showed signs of cytotoxicity at 10 μM, biphenyl **12t** and mono-TBS derivative **14** (CC_{50} = 7.5 and 5.8 μM, respectively, Table 1). Note that **12d**,**n**,**t** showed high permeability in the Caco-2 assay (Table 1) and that **12u**,**v** combine medium permeability in the Caco-2 assay with excellent stability when incubated with human liver microsomes for 30 min at 37 °C (**12u**, 94% parent compound remaining (PCR), and **12v**, 94% PCR).[20]

X-ray Crystallographic Data. The arrangement of benzyl bromide compounds **12d** (PDB code 2uxz), **15** (PDB code 2uy0), and **B** (PDB code 2bqv) in the active site of the HIV-1 protease including the most relevant hydrogen bonds to the enzyme amino acid residues, as deduced from X-ray crystallography, is presented in Figure 2. The complexes with **12d** and **15** were determined to 1.75 and 1.76 Å resolution and with R/R_{free} of 0.26/0.29 and 0.23/0.25, respectively. The largest compound, as expected, has the highest number of interactions with the protease. Thus, **15** makes 60 contacts within 3.9 Å to

Table 1. Antiviral Activity and Cytotoxicity of Compounds **12a–w** and **13−15**[a]

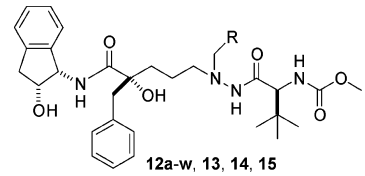

Cmpd	R-group	K_i[b] (nM)	EC_{50}[c] (μM)	CC_{50} (μM)
A	-	5.0	0.18	>10
12a[d]	Ph	5.7	1.20	>10
12b	4-F-Ph	6.7	0.98	>10
12c	4-Cl-Ph	3.4	0.91	>10
12d[d]	4-Br-Ph	3.3	0.85	>10
12d[e]	4-Br-Ph	420	>10	>10
12e	4-CN-Ph	2.9	1.20	>10
12f	4-NMe_2-Ph	4.9	0.98	>10
12g	$CH(CH_3)_2$	6.8	1.80	>10
12h	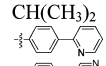	2.8	0.47	>10
12i	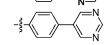	2.4	0.22	>10
12j	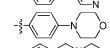	3.6	0.50	>10
12k	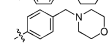	11	0.88	>10
12l	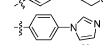	3.3	0.17	>10
12m	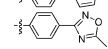	3.6	0.19	>10
12n[d]	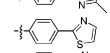	2.3	0.21	>10
12o		3.5	0.51	>10
12p	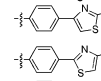	24	1.00	>10
12q	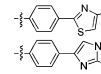	2.3	0.48	>10
12r		5.5	0.60	>10
12s	4-I-Ph	4.5	0.82	>10
12t[d]	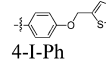	7.3	0.78	7.5
12u[d]	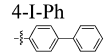	3.6	0.19	>10
12v[d]		2.8	0.17	>10
12w	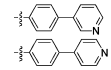	10	0.56	>10
13[f]	4-Br-Ph	980	>10	>10
14[g]	4-Br-Ph	190	>10	5.8
15[h]	4-Br-Ph	120	>10	>10

[a] All K_i values of novel structures were determined by two independent measurements. For biological activity determination methods and control of assay variability, see Supporting Information pages S17–S18. [b] Indinavir: K_i = 0.52 nM.[21] Atazanavir: K_i = 2.7 nM.[22] [c] Indinavir: EC_{50} = 0.041 μM.[23,24] Atazanavir: EC_{50} = 0.0039 μM.[22] [d] Inhibitors **12a**,**u**,**v** show medium permeability (3×10^{-6} cm/s < P_{app} < 20×10^{-6} cm/s), while **12d**,**n**,**t** show high permeability (P_{app} > 20×10^{-6} cm/s) in the Caco-2 assay.[20] Indinavir and saquinavir have previously been found to have low permeability,[25] while ritonavir[25] and atazanavir[8] have medium permeability. [e] *S*-configuration at the tertiary alcohol. [f] Both alcohols TBS-protected. [g] Only the tertiary alcohol TBS-protected. [h] Central diacylhydrazine unit.

the protein, **12d** makes 54 contacts, and **B** makes 48 contacts. Compound **12d** forms five hydrogen bonds directly to the protein and three via water molecules. The corresponding numbers for **15** and **B** are 7:5 and 8:3 (Figure 2). Because of the elongated central carbon skeleton of **12d** and **15** compared to **B**, the central hydroxyl of **12d** and **15** can only form a hydrogen bond to one of the active site aspartate residues. In contrast, the shorter **B** forms hydrogen bonds to both of the aspartate residues, even though the bond to Asp125 is weak (3.3 Å). The para bromo atom at the P1′ benzyl group is directed toward the solvent in inhibitor **12d** and **15** despite that the orientation of the P1′ groups differs. The orientation of P1′ side chain in **12d** corresponds to the pyridyl-substituted homologues of **B**.[9] In inhibitor **B** the bromine forms four close-packing

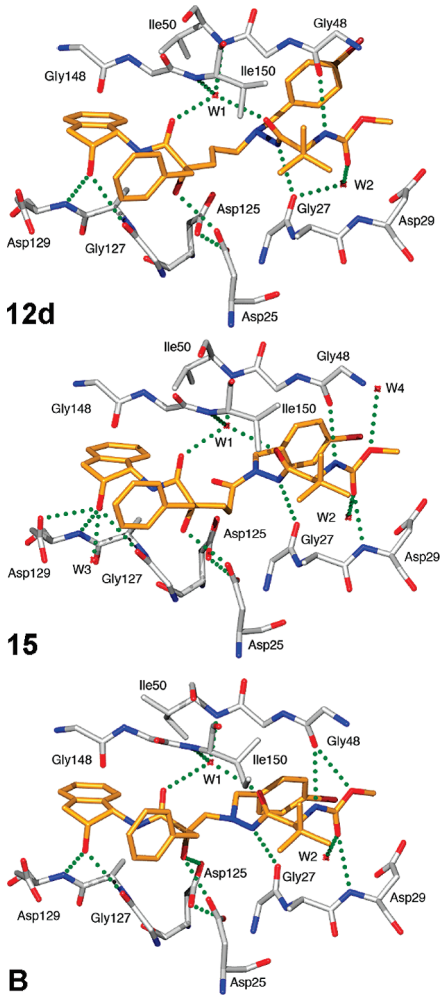

Figure 2. X-ray structures of **12d**, **15**, and **B** cocrystallized with the HIV-1 protease. The arrangement in the active site of HIV-1 protease is presented. Whereas the shorter central carbon skeleton of **B** enables hydrogen bonding of the central hydroxyl to the two active site residues Asp25 and Asp125, the longer central tether of **12d** and **15** allows only bonding to one of the Asp residues. The extra carbonyl oxygen in **15** is not involved in hydrogen-bonding to the protein. For large size X-ray structures of **12d**, **15**, and **B**, see Supporting Information, page S19.

contacts to the lining residues. The extra central carbonyl oxygen in diacylhydrazine **15** can function as a hydrogen-bond acceptor at low pH, when the catalytic aspartates are protonated, but at neutral pH the partially negatively charged carbonyl oxygen will be repelled by the negative charge of the aspartate oxygen. This is also reflected in a 40 times higher K_i for **15** compared to those for **12d** and **B**. Compared with the X-ray of indinavir (PDB code 1hsg), the novel structure **12d** is not as symmetrically positioned in the protease as indinavir. Indinavir has close contact (2.6–3.0 Å) interaction with Asp25 and 125, whereas **12d** has a close interaction with only Asp25 (2.9 Å). The distance to Asp 125 is 3.8 Å.

Discussion

The small variations in K_i obtained from the P1′ varied analogues indicate a high tolerability of the enzyme's S1′ pocket toward large differences in size and polarity of the corresponding inhibitor side chain.[26] A surprisingly high activity was attained for **14**, with an OTBS group instead of the free tertiary alcohol in the transition-state mimic (190 nM, Table 1). In the present study and in previous reports,[8,9] the importance of the tertiary alcohol has been clearly indicated by X-ray data, revealing the presence of hydrogen bonds to one of the catalytically active aspartic acid residues. Protected by the large TBS group, difficulties in forming the same type of hydrogen bonds should be apparent. Unfortunately, no attempt to obtain X-ray data for **14** in the active site of the enzyme to explain this feature was successful. The large difference in K_i between the *S*- and *R*-isomers (more than a 100-fold) was expected. However, the "wrong" *S*-diastereomer with $K_i = 420$ nM is still a fairly potent inhibitor of the HIV-1 protease. This could be interpreted by assuming a different binding mode to the enzyme for the two isomers, which have been postulated in the case of aspartic protease inhibitors (not including HIV-1) by Rich et al.[27–29] Notably, **A** and **12u**, which only differ in the length of the transition-state mimicking scaffold, have a very small variance in K_i, equal to 1.4 nM (Table 1). This can be partly explained by the data obtained from X-ray crystallography, where the short **B** is compared with the elongated structure **12d**, both with the bromobenzene group in P1′ (Figure 2). As mentioned, both structures interact with the enzyme in a similar way and both compounds have a strong interaction with Asp25. The lack of a weak hydrogen bond to Asp125 for structure **12d** compared to **B** does not seem to affect the K_i. The cellular antiviral activities were clearly more influenced by the nature of the P1′ substituent compared to the K_i. Biaryl groups with a relatively hydrophilic heterocyclic second ring structure seem to be preferred to gain good activity. We have previously reported that the pyridines as P1′ substituents increase cell-based activity notably compared to other evaluated groups.[9] However, in this study we were able to present alternative groups, such as the pyrimidine, imidazole, and oxadiazole units, delivering equipotent compounds in these assays (**12i**,**l**,**m**, Table 1).

Conclusion

Within the area of HIV-1 protease inhibitors containing a tertiary-alcohol-based transition-state mimic, we have presented new compounds with a two-carbon-elongated core structure. Compared to previous studies, we have extended the SAR of the P1′ group by synthesizing 23 analogues, investigating small to large P1′ side chains with different polarity and hydrogen-bonding potential. We were able to identify three new terminal P1′ substituents, a pyrimidine, an imidazole, and an oxadiazole, as good competitors of the known pyridines in achieving improved antiviral activity in cell culture. The best pyridine compound within the series, **12v**, was also an overall more potent inhibitor of the HIV-1 protease, with $K_i = 2.8$ nM and $EC_{50} = 0.17$ μM. X-ray crystal data revealed the binding mode for benzyl bromide inhibitors **12d** and **15**.

Experimental Section

General Procedure B for Synthesis of Inhibitors 12a–c and 12e–s. Dry CH_2Cl_2 (15 mL) was added to alcohol (*R*)-**6** (1.0–2.0 equiv) and Dess−Martin reagent (1.05–2.2 equiv). The solution was stirred at room temperature for 1 h and then concentrated, and the residue was dissolved in Et_2O (15 mL), washed with saturated $NaHCO_3$ (aq, 15 mL) and saturated $Na_2S_2O_3$ (aq, 4 mL). The aqueous layers were extracted with Et_2O (2 × 15 mL). The ether layers were combined, dried ($MgSO_4$), and concentrated to yield the crude aldehyde. Hydrazide **9** (1.0 equiv) and AcOH (1.7–2.6 equiv) in THF (10 mL) were added to the aldehyde and stirred for 15 min at room temperature. $Na(OAc)_3BH$ (3.3–4.0 equiv) was added, and the mixture was stirred at room temperature overnight. The reaction was quenched with saturated NH_4Cl (aq), extracted with CH_2Cl_2 (3 × 20 mL), dried ($MgSO_4$), and concentrated. Purification by flash chromatography was performed, and the fractions with desired mass value were combined and concentrated to give the crude product with TBS protected

alcohol groups. TBAF (3.5–10.0 equiv based on the amount of starting material **9**) in THF was added to the intermediate and stirred overnight. Purification by flash chromatography gave the corresponding products **12a–c** and **12e–s** as white solids in yields varying from 19% to 91%.

General Procedure C for Synthesis of Inhibitors 12t–w. Palladium-Catalyzed Coupling Reactions. Aryl bromide **13** (1.0 equiv), boronic acid (3.0 equiv), Herrmann's palladacycle (0.05 equiv), HP(*t*-Bu)$_3$BF$_4$ (0.10 equiv), K_2CO_3 (3.0 equiv), DME, and H_2O were added to a 2–5 mL process vial. The mixture was radiated under microwaves at 120 or 130 °C for 20 min. The mixture was then extracted with EtOAc, and the organic layer was dried ($MgSO_4$) and concentrated. TBAF (1.0 M in THF, 10.0 equiv) was added to the residue and stirred at room temperature overnight. Water (10 mL) was added to the mixture, followed by extraction with CH_2Cl_2, drying ($MgSO_4$), concentration, and purification on silica to afford the products **12t**−**w** as white solids in 61–80% yield.

{(*S*)-1-[*N*′-[(*R*)-4-Hydroxy-4-((1*S*,2*R*)-2-hydroxy-indan-1-ylcarbamoyl)-5-phenylpentyl]-*N*′-(4-pyridin-4-ylbenzyl)hydrazinocarbonyl]-2,2-dimethylpropyl}carbamic Acid Methyl Ester (12v). The title compound was made according to general procedure C, using **13** (100.0 mg, 0.1066 mmol), 4-pyridinylboronic acid (39.2 mg, 0.3198 mmol), palladacycle (5.0 mg, 0.0053 mmol), HP(*t*-Bu)$_3$BF$_4$ (3.1 mg, 0.0107 mmol), K_2CO_3 (44.2 mg, 0.3198 mmol), DME (1.0 mL), and H_2O (0.3 mL), which were radiated at 120 °C for 20 min. TBAF (1.0 M in THF, 1.06 mL, 1.06 mmol) was used for deprotection. Purification (silica, MeOH/CH_2Cl_2, 1:99 to 5:95) gave **12v** (52.9 mg, 70%). ^{1}H NMR (CD_3OD, 400 MHz) δ 0.75 (s, 9H), 1.56–1.70 (m, 1H), 1.70–1.86 (m, 2H), 2.03–2.16 (m, 1H), 2.74–2.94 (m, 4H), 3.01–3.14 (m, 2H), 3.46 (s, 3H), 3.70 (s, 1H), 3.88–4.00 (m, 2H), 4.16–4.22 (m, 1H), 5.09 (d, J = 4.8 Hz, 1H), 7.10–7.30 (m, 9H), 7.50–7.70 (m, 6H), 8.50–8.60 (m, 2H); MS (*m*/*z* 708, M + H$^+$). Anal. ($C_{41}H_{49}N_5O_6 \cdot H_2O$) C, H, N.

Acknowledgment. We thank the Swedish Research Council (VR) and the Swedish Foundation for Strategic Research (SSF) for financial support, Seved Löwgren for help with preparation of the protease, and Dr. Yogesh Sabnis for help with the manuscript.

Note Added after Print Publication. To correct a printing error related to Scheme 3, this paper was reposted on March, 14, 2008.

Supporting Information Available: Experimental details and spectroscopic data for **2–15**, elemental analysis data, X-ray structure determination details, and procedures for enzyme assay. This material is available free of charge via the Internet at http://pubs.acs.org.

References

(1) *AIDS Epidemic Update: December 2006*; Joint United Nations Programme on HIV/AIDS (UNAIDS/WHO): Geneva, 2006.
(2) Brik, A.; Wong, C.-H. HIV-1 protease: mechanism and drug discovery. *Org. Biomol. Chem.* **2003**, *1*, 5–14.
(3) Randolph, J. T.; DeGoey, D. A. Peptidomimetic inhibitors of HIV protease. *Curr. Top. Med. Chem.* **2004**, *4*, 1079–1095.
(4) Abdel-Rahman, H. M.; Al-Karamany, G. S.; El-Koussi, N. A.; Youssef, A. F.; Kiso, Y. HIV protease inhibitors: peptidomimetic drugs and future perspectives. *Curr. Med. Chem.* **2002**, *9*, 1905–1922.
(5) Rodríguez-Barrios, F.; Gago, F. HIV protease inhibition: limited recent progress and advances in understanding current pitfalls. *Curr. Top. Med. Chem.* **2004**, *4*, 991–1007.
(6) Clavel, F.; Hance, A. J. HIV drug resistance. *N. Engl. J. Med.* **2004**, *350*, 1023–1035.
(7) de Mendoza, C.; Soriano, V. Resistance to HIV protease inhibitors: mechanisms and clinical consequences. *Curr. Drug Metab.* **2004**, *5*, 321–328.
(8) Ekegren, J. K.; Unge, T.; Safa, M. Z.; Wallberg, H.; Samuelsson, B.; Hallberg, A. A new class of HIV-1 protease inhibitors containing a tertiary alcohol in the transition-state mimicking scaffold. *J. Med. Chem.* **2005**, *48*, 8098–8102.
(9) Ekegren, J. K.; Ginman, N.; Johansson, Å.; Wallberg, H.; Larhed, M.; Samuelsson, B.; Unge, T.; Hallberg, A. Microwave accelerated synthesis of P1′-extended HIV-1 protease inhibitors encompassing a tertiary alcohol in the transition-state mimicking scaffold. *J. Med. Chem.* **2006**, *49*, 1828–1832.
(10) Ekegren, J. K.; Gising, J.; Wallberg, H.; Larhed, M.; Samuelsson, B.; Hallberg, A. Variations of the P2 group in HIV-1 protease inhibitors containing a tertiary alcohol in the transition-state mimicking scaffold. *Org. Biomol. Chem.* **2006**, *4*, 3040–3043.
(11) Winneroski, L. L.; Xu, Y. Two complementary approaches toward 2-alkoxy carboxylic acid synthesis from 1,3-dioxolan-4-ones. *J. Org. Chem.* **2004**, *69*, 4948–4953.
(12) Bold, G.; Fässler, A.; Capraro, H.-G.; Cozens, R.; Klimkait, T.; Lazdins, J.; Mestan, J.; Poncioni, B.; Rösel, J.; Stover, D.; Tintelnot-Blomley, M.; Acemoglu, F.; Beck, W.; Boss, E.; Eschbach, M.; Hurlimann, T.; Masso, E.; Roussel, S.; Ucci-Stoll, K.; Wyss, D.; Lang, M. New aza-dipeptide analogues as potent and orally absorbed HIV-1 protease inhibitors: candidates for clinical development. *J. Med. Chem.* **1998**, *41*, 3387–3401.
(13) Otteneder, M.; Plastaras, J. P.; Marnett, L. J. Reaction of malondialdehyde−DNA adducts with hydrazines—development of a facile assay for quantification of malondialdehyde equivalents in DNA. *Chem. Res. Toxicol.* **2002**, *15*, 312–318.
(14) Kappe, C. O.; Dallinger, D. The impact of microwave synthesis on drug discovery. *Nat. Rev. Drug Discovery* **2006**, *5*, 51–63.
(15) Larhed, M.; Moberg, C.; Hallberg, A. Microwave-accelerated homogeneous catalysis in organic chemistry. *Acc. Chem. Res.* **2002**, *35*, 717–727.
(16) Larhed, M.; Wannberg, J.; Hallberg, A. Controlled microwave heating as an enabling technology: expedient synthesis of protease inhibitors in perspective. *QSAR Comb. Sci.* **2007**, *26*, 51–68.
(17) Ersmark, K.; Larhed, M.; Wannberg, J. Microwave-enhanced medicinal chemistry: a high-speed opportunity for convenient preparation of protease inhibitors. *Curr. Opin. Drug Discovery Dev.* **2004**, *7*, 417–427.
(18) Herrmann, W. A.; Bohm, V. P. W.; Reisinger, C.-P. Application of palladacycles in Heck type reactions. *J. Organomet. Chem.* **1999**, *576*, 23–41.
(19) Miller, J. F.; Andrews, C. W.; Brieger, M.; Furfine, E. S.; Hale, M. R.; Hanlon, M. H.; Hazen, R. J.; Kaldor, I.; McLean, E. W.; Reynolds, D.; Sammond, D. M.; Spaltenstein, A.; Tung, R.; Turner, E. M.; Xu, R. X.; Sherrill, R. G. Ultra-potent P1 modified arylsulfonamide HIV protease inhibitors: the discovery of GW0385. *Bioorg. Med. Chem. Lett.* **2006**, *16*, 1788–1794.
(20) Medivir data.
(21) Dorsey, B. D.; Levin, R. B.; McDaniel, S. L.; Vacca, J. P.; Guare, J. P.; Darke, P. L.; Zugay, J. A.; Emini, E. A.; Schleif, W. A.; Quintero, J. C.; Lin, J. H.; Chen, I.-W.; Holloway, M. K.; Fitzgerald, P. M. D.; Axel, M. G.; Ostovic, D.; Anderson, P. S.; Huff, J. R. L-735,524: the design of a potent and orally bioavailable HIV protease inhibitor. *J. Med. Chem.* **1994**, *37*, 3443–3451.
(22) Robinson, B. S.; Riccardi, K. A.; Gong, Y.-F.; Guo, Q.; Stock, D. A.; Blair, W. S.; Terry, B. J.; Deminie, C. A.; Djang, F.; Colonno, R. J.; Lin, P.-F. BMS-232632, a highly potent human immunodeficiency virus protease inhibitor that can be used in combination with other available antiretroviral agents. *Antimicrob. Agents Chemother.* **2000**, *44*, 2093–2099.
(23) Randolph, J. T.; DeGoey, D. A. Peptidomimetic inhibitors of HIV protease. *Curr. Top. Med. Chem.* **2004**, *4*, 1079–1095.
(24) Molla, A.; Vasavanonda, S.; Kumar, G.; Sham, H. L.; Johnson, M.; Grabowski, B.; Denissen, J. F.; Kohlbrenner, W.; Plattner, J. J.; Leonard, J. M.; Norbeck, D. W.; Kempf, D. J. Human serum attenuates the activity of protease inhibitors toward wild-type and mutant human immunodeficiency virus. *Virology* **1998**, *250*, 255–262.
(25) Williams, G. C.; Sinko, P. J. Oral absorption of the HIV protease inhibitors: a current update. *Adv. Drug Delivery Rev.* **1999**, *39*, 211–238.
(26) Alterman, M.; Andersson, H. O.; Garg, N.; Ahlsen, G.; Lövgren, S.; Classon, B.; Danielson, U. H.; Kvarnström, I.; Vrang, L.; Unge, T.; Samuelsson, B.; Hallberg, A. Design and fast synthesis of C-terminal duplicated potent C_2-symmetric P1/P1′-modified HIV-1 protease inhibitors. *J. Med. Chem.* **1999**, *42*, 3835–3844.
(27) Rich, D. H. Pepstatin-derived inhibitors of aspartic proteinases. A close look at an apparent transition-state analog inhibitor. *J. Med. Chem.* **1985**, *28*, 263–273.
(28) Rich, D. H.; Bernatowicz, M. S.; Agarwal, N. S.; Kawai, M.; Salituro, F. G.; Schmidt, P. G. Inhibition of aspartic proteases by pepstatin and 3-methylstatine derivatives of pepstatin. Evidence for collected-substrate enzyme inhibition. *Biochemistry* **1985**, *24*, 3165–3173.
(29) Agarwal, N. S.; Rich, D. H. Inhibition of cathepsin D by substrate analogs containing statine and by analogs of pepstatin. *J. Med. Chem.* **1986**, *29*, 2519–2524.

JM070680H